Biological, Medical Devices, and Systems

Microfluidics and Computational Imaging for Measuring Cells' Intrinsic Properties

N. Apichitsopa, J. Voldman
Sponsorship: Bose Research Award

Scientific-grade optical microscopes are very powerful tools in the field of microfluidics as they can be used to observe the behaviors of micro-objects of interest inside the microfluidic devices. While conventional optical microscopes are limited by the small field of view (FOV), e.g., ~1-2 mm^2 for a 10X objective, the footprint of a microfluidic platform is typically ~cm^2. This mismatch of the FOV of the microscope and the footprint of the device restricts the area of the device and the number of micro-objects that can be viewed at the same specific time points. Although mechanically moving and observing different areas of the device under the microscope is acceptable for objects with fewer dynamic movements, it is not suitable for objects with fast movement in large-footprint particle separation devices.

Computational microscopy has been shown to provide large FOV with an order of magnitude larger than the 10X objective. We propose to combine visual observation from large FOV computational microscopy with separation of cells via a label-free microfluidic platform in order to study cell size. This system will benefit from the parallel and gentle separation of label-free cells via a microfluidic platform and parallel tracking of multiple cells in a large FOV, in contrast to the gold standard, flow cytometry, which is able to rapidly identify properties of cells in a single stream via emittance of external fluorescent cell markers. A prototype of the integrated platform was designed and fabricated. The prototype consists of a digital in-line holographic microscopy system (Figure 1) and a microfluidic deterministic lateral displacement array, which separates particles based on size. Each system was first characterized separately and later integrated, so that individual cells inside the deterministic lateral displacement array could be recorded and tracked with the large FOV digital in-line holographic microscopy system (Figure 2).

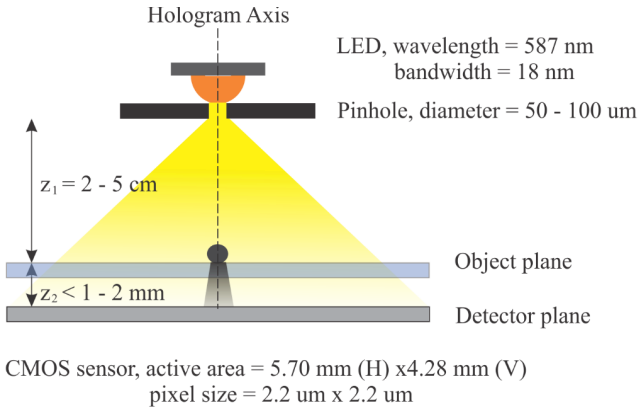

▲ Figure 1: Schematic of the large-FOV digital in-line holography system.

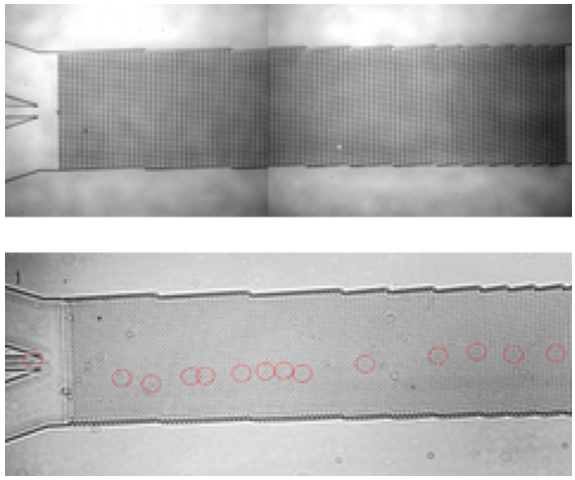

▲ Figure 2: Stitched microscope images of the deterministic lateral displacement array system (top) and the recorded holograms from the same device as cells flowed from left to right (bottom). Red circles depict detected cells.

FURTHER READING

- O. Mudanyali, D. Tseng, C. Oh, S. Isikman, I. Sencan, W. Bishara, C. Oztoprak, S. Seo, B. Khademhosseini, and A. Ozcan, "Compact, Light-Weight and Cost-Effective Microscope Based on Lensless Incoherent Holography for Telemedicine Applications," *Lab Chip*, vol. 10, no. 11, 1417–1428, Jun. 2010.
- L. R. Huang, E. C. Cox, R. H. Austin, and J. C. Sturm, "Continuous Particle Separation through Deterministic Lateral Displacement," *Science*, vol. 304, no. 5673, 987–990, 2004.

Microfluidic and Electronic Detection of Protein Biomarkers

D. Wu, J. Voldman
Sponsorship: Analog Devices, Inc.

Measuring proteins biomarkers in blood is of significant clinical importance and has a substantial market. However, traditional blood tests performed in centralized laboratories take days to deliver results to patients. The need for large volumes (~mL) of blood samples also makes it challenging to perform testing of newborns and even premature infants, who have very limited blood. We are developing a bead-based microfluidic electronic biosensor that gives immediate results and requires a small volume (μL) of blood, potentially allowing testing of neonates.

The biosensor is illustrated in Figure 1 after magnetic microbeads conjugated with antibodies and enzymes are added to the sample, the biomarkers bind to antibodies because of the specific interaction between proteins and antibodies. The use of magnetic microbeads shortens the diffusion length of proteins to antibodies and thus significantly accelerates the binding process. The magnetic beads are then sent to the sensor, which consists of microfluidic channels and microelectrodes, and eventually attach to the antibodies immobilized on electrodes. The enzymes on microbeads catalyze chemical reactions and generate current, which is measured by external electronics. The amount of protein in the original sample is associated with the measured current. Figure 2 shows the results of measuring human IL-6 (~22 kDa). The results indicate that the sensitivity of our sensor is about 1 pg/mL, which is sufficient to measure most of the protein biomarkers in blood.

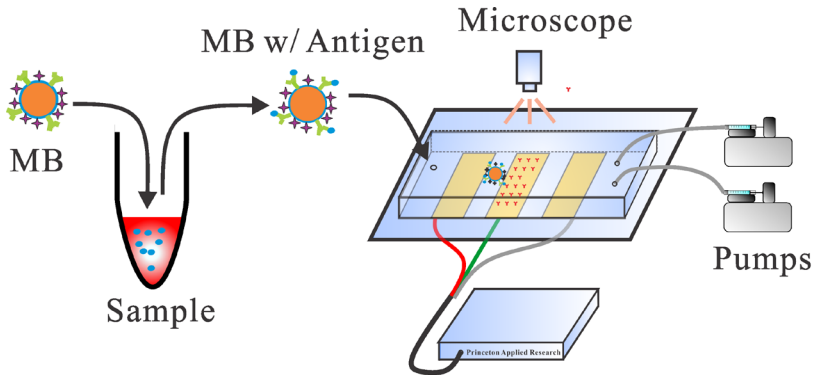

▲ Figure 1: Illustration of the biosensor.

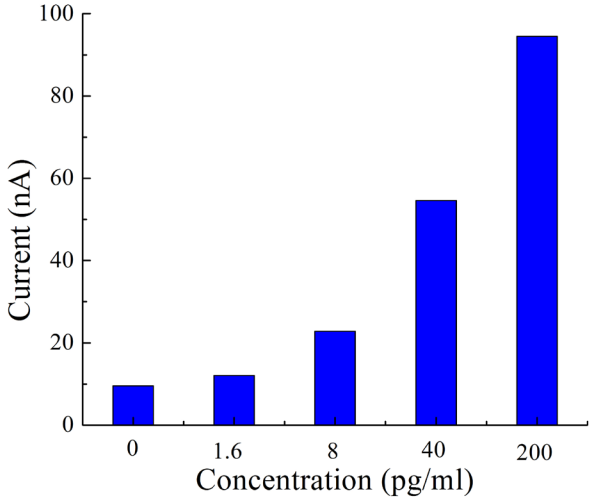

▲ Figure 2: Results of measuring human IL -6.

A Cell-Counting System for Point-of-Care Blood and Urine Analysis

S. R. Primas, C. G. Sodini
Sponsorship: MEDRC, Analog Devices, Inc.

Quantifying the concentration of medically relevant cells in blood and urine remains one of the most in-demand diagnostic techniques in medicine. For example, complete blood counts (CBCs) are conducted at nearly every medical checkup to monitor diseases ranging from anemia to chronic inflammatory diseases to HIV. And, with urine, cell-counting is used to conclusively determine bacteria concentrations for the detection of urinary tract infections (UTIs). UTIs lead to 6.7 million physician office visits and 2.6 million ER visits per year in the United States.

Due to the cost and complexity of blood and urine cell counts, the majority are conducted at a medical lab instead of at the point-of-care. These labs use either expensive flow-cytometers (e.g., the Sysmex UF-1000i is $125,000) or manual classification by trained professionals using a microscope. An inexpensive and automated cell-counting system would significantly increase the access to these important diagnostic tests and even enable them to be performed at the point-of-care.

This project focuses on developing both automated cell classification and an inexpensive image acquisition system. For the automated classification, the system uses a 7-layer convolutional neural network in TensorFlow to differentiate among six categories of particles observed in urine: bacteria, red blood cells, sperm, white blood cells, crystals, and an "other" category (see Figures 1 and 2). To obtain images at a low cost with a sufficiently high resolution, we use a reversed lens approach. By adding a reversed lens onto the original lens (<$6US for the lenses), we achieve a field-of-view equivalent to the size of the image sensor while maintaining a pixel resolution between 0.9-1.2um/pixel (depending on the pixel density of the image sensor). By combining these approaches, we hope to demonstrate a proof-of-concept of a low-cost cell-counting system for point-of-care applications.

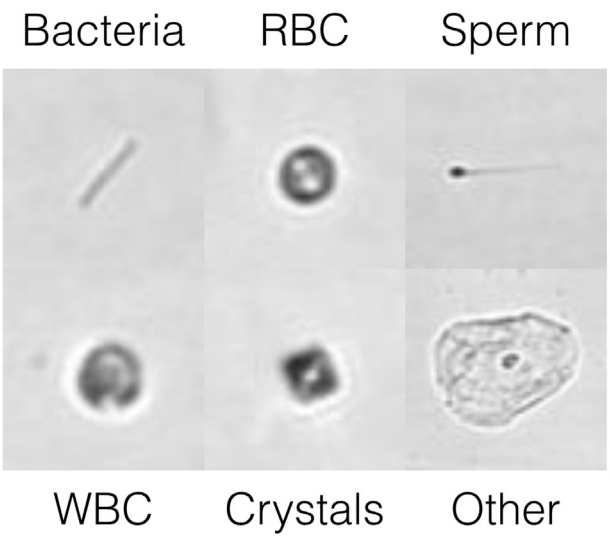

▲ Figure 1: Microscopic images of particles found in urine. These are pre-labeled reference images used to train the convolutional neural network and validate functionality.

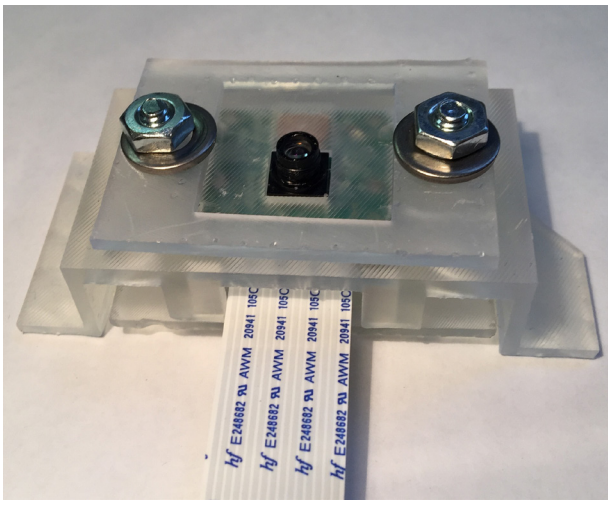

▲ Figure 2: The image acquisition device includes a 5-megapixel CMOS image sensor (OV5647), a reversed lens setup, and a jig used to control the distance between the object and the lens.

FURTHER READING

- N. A. Switz, M. V. D'Ambrosio, and D. A. Fletcher, "Low-Cost Mobile Phone Microscopy with a Reversed Mobile Phone Camera Lens," *PloS One*, vol. 9, no. 5, e95330, 2014.
- M. Ranzato, et al., "Automatic Recognition of Biological Particles in Microscopic Images," *Pattern Recognition Lett.*, vol. 28, no. 1, 31-39, 2007.

Amplification-Free Nucleic Acid Analysis for Point-of-Care Tuberculosis Diagnostics

W. Ouyang, J. Han
Sponsorship: NIH

Tuberculosis (TB) is one of the world's most widely spread diseases, with one third of the global population being infected. In 2014, 9.6 million people fell ill with TB and 1.5 million died from the disease, 95% of which occurred in developing countries. While a total of 150 millions TB tests (including 80 million point-of-care tests) are ordered each year, most existing TB diagnostic methods—microscopy, culture, or nucleic acid amplification tests—do not match all the Affordable Sensitive Specific User-friendly, Rapid/Robust, Equipment-free, Deliverable (ASSURED) criteria for the resource-poor milieu where most infections occur. In this work, we aim to develop a rapid (<30 min) nucleic acid-based diagnostic platform without engaging the commonly used nucleic acid amplification process, which is expensive, complicated, prone to false positives, and requires trained personnel. This goal will be achieved by a billion-fold microfluidic electrokinetic concentrator that dramatically increases the local concentration of nucleic acids, in which a simple assay is concurrently performed to recognize target nucleic acids with specific sequences.

We have previously demonstrated a microfluidic electrokinetic concentrator that can enrich negatively-charged molecules by ten thousand fold within 15 minutes. We are now working on a multi-stage concentrator that performs a first-stage concentration with thousands of the aforementioned concentrators, followed by a second-stage concentration that collects and concentrates the first-stage concentrated molecules, thereby significantly increasing the overall concentration capability. Our primary results in a two-stage (16-1) concentrator indicates that we could increase the concentration factor from ~10^4 to ~10^5 (Figure 1). We will further scale up by introducing thousands of channels in the first stage to further push the concentration performance. To detect nucleic acid specific to TB, we have developed a mobility shift assay in the concentrator with a limit of detection of ~1 pM. TB patient DNA samples were incubated with a fluorescent complementary DNA probe. During testing in the concentrator, the target-probe and probe formed two separate peaks due to different electrical mobility, enabling us to quantify the level of TB DNA in the sample. By further increasing the concentration capacity of the concentrator, we can hopefully lower the limit of detection to sub-femtomolar.

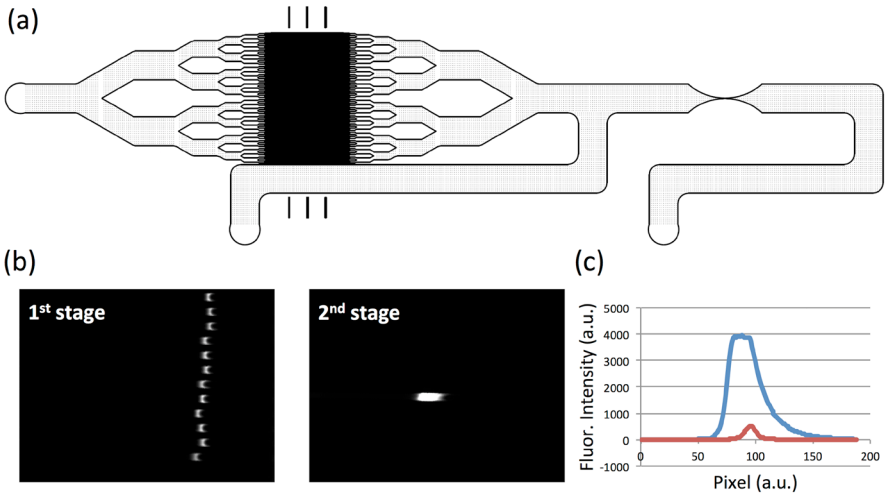

▲ Figure 1: (a) Design of a two-stage microfluidic electrokinetic concentrator. (b) Fluorescence images of the concentration plugs in the first and second stages. (c) Comparison of the concentration plug in the first (purple) and second (blue) stages.

FURTHER READING

- W. Ouyang, S. H. Ko, D. Wu, A. Y. Wang, P. W. Barone, W. S. Hancock, and J. Han, "Microfluidic Platform for Assessment of Therapeutic Proteins using Molecular Charge Modulation Enhanced Electrokinetic Concentration Assays," *Analytical Chemistry*, vol. 88, 9669-9677, 2014.
- L. F. Cheow and J. Han, "Continuous Signal Enhancement for Sensitive Aptamer Affinity Probe Electrophoresis Assay using Electrokinetic Concentration," *Analytical Chemistry*, vol. 83, 7086, 2011.

Nanofluidic Transport of Molecules in Enamels by Electrokinetic Flows

C. Peng, J. Han, in collaboration with H.-Y. Gan, F. Sousa, S. Park, S. J. Lee
Sponsorship: Colgate

The ability to infiltrate various molecules and resins into dental enamel is highly desirable in dentistry, yet transporting materials into dental enamel is limited by the nanometric scale of their pores, as Figure 1 shows. Materials that cannot be infiltrated into enamel by diffusion/capillarity may have molecules that are larger than a critical threshold, perhaps the size of the pores of enamel. It has been demonstrated that electrokinetic flow has been adopted to improve the infiltration of molecules and resin to the dental enamal. Figure 1 shows the preliminary published results of such use of electrokinetic flow to infiltrate enamel.

In the current work, the enamel ground sections are prepared by removing dentin from the tooth ground sections and seated in the microfluidic platform. We study the infiltration of different ion molecules such as Ca^{2+}, K^{+}, and Na^{+} into the enamel nanopores by using electrokinetic flows. We have demonstrated that the fluorescence probes binding to the specific ions have been transported through the enamel. Meanwhile, the current change in this process has been monitored, and it shows that the current increases during the infiltration due to the increasing overall conductivity. Laser scanning confocal microscope images of the enamel cross-section demonstrate that the fluorescence probes binding to the ions have infiltrated into the nanopores of the enamel. Micro-hardness tests (Vickers) and nano-indentation trials have been carried out by our collaborators on trial samples of both whole teeth and grounded sheets of enamel.

We study the improved health of the whole tooth due to use of resin infiltration using electrokinetics, which will be a big boost to clinical care in the near future. This study is the first demonstration that resin can be infiltrated through the enamel and dentin nanopores. By using laser scanning confocal microscopy, fluorescence microscopy, mass spectroscopy, and ion selective electrode technique, we will test how the F^{-}, Na^{+}, K^{+}, and Ca^{2+} ions infiltrate into the teeth. Micro-hardness and chemical resistance of the teeth after the resin polymerization will be tested. This will be a very promising technique to improve dental health in a very short time and will shed light on future *in vivo* utility in the clinic. This technique might be a solution to the weak bonding between filling resin and pulp-dentin-enamel surfaces after treatment of cavities.

This study opens opportunities to use a new biomedical technique in dental applications and may find utility in clinical dental treatments.

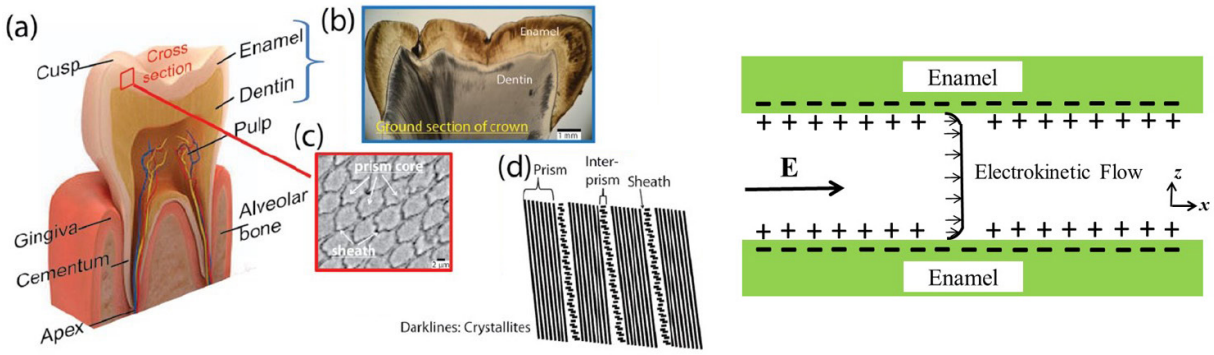

▲ Figure 1: Diagram of enamel and its pores. (a) Anatomy of a mature human tooth. (b) Light microscopy image of ground section of tooth crown showing enamel, dentin, enamel-dentin junction, and an outline of enamel prisms. (c) Cross section of enamel prisms showing prism core and sheaths, and (d) Line drawing of hydroxyapatite crystallites as oriented in prismatic and interprismatic enamel separated by prism sheaths. Right: Schematic of electrokinetic flow inside the enamel nanopores.

FURTHER READING

- H. Y. Gan, F. Sousa, H. L. Carlo, P. P. Maciel, M. S. Macena, and J. Han, "Enhanced Transport of Materials into Enamel Nanopores via Electrokinetic Flow," *J. Dental Research,* vol. 94, 0615-621, 2015.

A Microfluidic Platform Enabling Single-Cell RNA-seq of Multigenerational Lineages

R. J. Kimmerling, G. L. Szeto, J. W. Li, A. S. Genshaft, S. W. Kazer, K. R, Payer, J. Borrajo, P. C. Blainey, D. J. Irvine, A. K. Shalek, S. R. Manalis
Sponsorship: NIH

We introduce a microfluidic platform that enables off-chip single-cell RNA-seq after multi-generational lineage tracking under controlled culture conditions. We use this platform to generate whole-transcriptome profiles of primary, activated murine CD8+ T-cell and lymphocytic leukemia cell line lineages. Here we report that both cell types have greater intra- than inter-lineage transcriptional similarity. For CD8 + T-cells, genes with functional annotation relating to lymphocyte differentiation and function—including Granzyme B—are enriched among the genes that demonstrate greater similarity of intra-lineage expression level. Analysis of gene expression covariance with matched measurements of time since division reveals cell type-specific transcriptional signatures that correspond with cell cycle progression. We believe that the ability to directly measure the effects of lineage and cell cycle-dependent transcriptional profiles of single cells will be broadly useful to fields where heterogeneous populations of cells display distinct clonal trajectories, including immunology, cancer, and developmental biology.

Our platform utilizes an array of hydrodynamic traps within a fluidic design optimized to capture and culture single cells for multiple generations on-chip (Figure 1). These trap structures rely on differences in hydrodynamic resistance between the trapping pocket and a bypassing serpentine channel to deterministically capture single cells. Given these differences, media can be rapidly and continuously perfused through the bypass channels while maintaining minimal flow across the traps in order to ensure constant nutrient repletion with low and uniform shear stress on the cells. This independent flow control also allows for rapid buffer exchange without dislodging trapped cells, thus enabling on-chip implementation of standard cell staining techniques such as immunocytochemistry and fluorescent labeling. Single cells were cultured for two generations on-chip before release for sequencing. This allowed us to define sister and cousin cell pairs for each lineage (Figure 2).

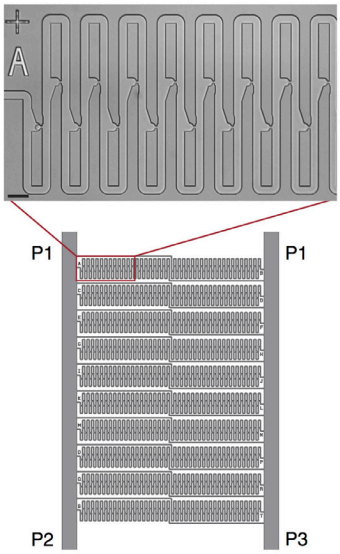

▲ Figure 1: Schematic representation of the hydrodynamic trap array consisting of 20 lanes of traps (inset shows an optical micrograph of a single trapped cell—scale bar, 20 μm).

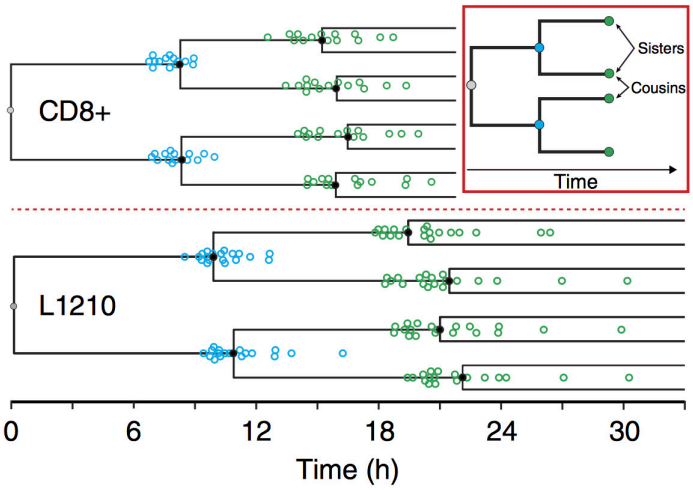

▲ Figure 2: Overlay of lineage trees from single CD8+ T cells (n=15) and L1210 cells (n=20) established with time-lapse imaging in the hydrodynamic trap array. As a demonstration of lineage construction, one lineage for each cell type (black circles) has connecting lines indicating familial history.

FURTHER READING

- R. J. Kimmerling, G. L. Szeto, J. W. Li, A. S. Genshaft, S. W. Kazer, K. R, Payer, J. Borrajo, P. C. Blainey, D. J. Irvine, A. K. Shalek, and S. R. Manalis, "A Microfluidic Platform Enabling Single-Cell RNA-Seq of Multigenerational Lineages," *Nature Communications*, vol. 10220, no. 7, 1-7, 2016.

3-D Printed Microfluidics for Modelling Tumor Microenvironments

A. L. Beckwith, J. T. Borenstein, L. F. Velásquez-García
Sponsorship: The Charles Stark Draper Laboratory, Inc.

Microfluidic devices show promise as enablers of the exploration, development, and customization of medical treatments beyond traditional capabilities while saving time and cost. However, one of the principal barriers to broad application of microfluidic technologies in healthcare is related to the inherent challenges in device fabrication. Soft lithography approaches are generally restricted to planar, simple geometries and a few material options and are prone to large device-to-device dimensional variation. Current manufacturing methods for complex microfluidic devices, e.g., multi-substrate bonded micromachining, are technically challenging, time-intensive, and constrained by existing microfabrication capabilities that affect the fabrication yield. 3-D printing has the potential to significantly reduce the cost and time to manufacture microfluidics while maintaining a required level of device functionality. Additionally, 3-D printing enables rapid iteration of device designs and construction of complex microchannel features that may otherwise be difficult, impractical, or unfeasible to attain.

In this project, we are developing a Tumor Analysis Platform (TAP) that mimics interactions between tumors and the immune system in the human body, providing a microenvironment for testing the effectiveness of drugs. This microfluidic system is capable of testing treatments on tumors directly from the patient in a laboratory model to determine which therapies most effectively kill that patient's cancer. We are investigating digital light projection/stereolithography (DLP/SLA) to fabricate complex monolithic microfluidic devices that are transparent, non-cytotoxic, compatible with commonly used sterilization procedures, and, in general, suitable for biological applications. Current research has focused on exploring the biocompatibility, optical properties, minimum feature size resolution, and manufacturing repeatability of different printable materials (Figures 1 and 2). Future work will focus on implementing and characterizing different TAP designs.

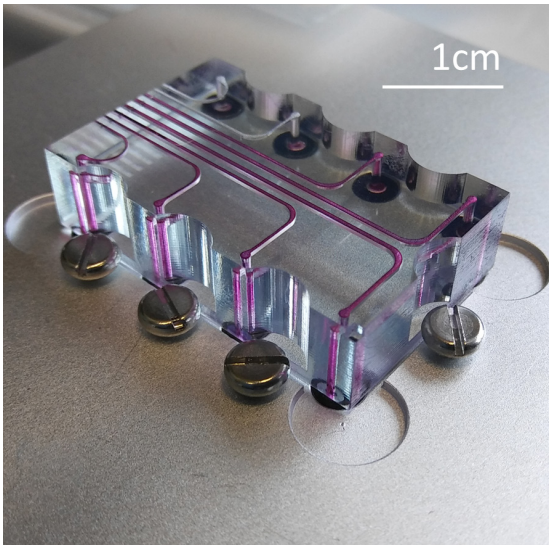

▲ Figure 1: SLA 3-D printed channels with rectangular cross-sections. Channel widths as small as 275 μm were successfully printed and filled with red dye.

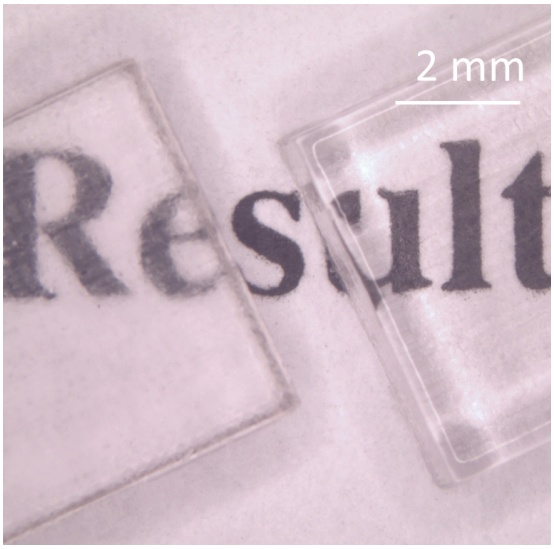

▲ Figure 2: Chip of 3-D printed material evidencing high transparency to visible light.

FURTHER READING

- L. F. Velásquez-García, "SLA 3-D-Printed Arrays of Miniaturized, Internally-Fed, Polymer Electrospray Emitters," *J. Microelectromechanical Systems*, vol. 24, no. 6, 2117-2127, 2015.
- D. Olvera-Trejo and L. F. Velásquez-García, "Additively Manufactured MEMS Multiplexed Coaxial Electrospray Sources for High-Throughput, Uniform Generation of Core-Shell Microparticles," *Lab Chip*, vol. 16, no. 21, 4121-4132, 2016.
- A. P. Taylor and L. F. Velásquez-García, "3-D Printed Miniaturized Diaphragm Vacuum Pump," *Technical Digest 30th IEEE Conference on Micro Electro Mechanical Systems (MEMS 2017)*, Jan. 2017.

Integration of Nanofluidics in Commercial CMOS

H. Meng, J. Kim, A. Atabaki, R. Ram
Sponsorship: Bose Corporation

Lab-on-complementary-metal-oxide-semiconductor (CMOS) is an emerging platform for bio-sensing applications. Integration of various sensors and active circuits into a single CMOS chip provides benefits including ultra-compact form factor, enhanced signal collection efficiency, reduction of noise and massively parallel sensing. Nanofluidics offers the ability to engineer systems with comparable complexity and scale to biomolecules and opens the door to a new generation of molecular tools. A novel approach to leverage the precision and scale of CMOS to integrate nanofluidics, nanophotonics, and nanoelectronics on the same platform is presented.

Nanofluidic channels are integrated within a modified IBM 65-nm (10LP) CMOS process. The nanofluidics are introduced by sacrificial etching of the polysilicon typically used for the transistor gate, for local interconnection, and for precision resistors. The polysilicon can be patterned at the critical dimension of the process (65 nm in our case), and the polysilicon features are routinely placed with an accuracy of approximately 1 nm. This polysilicon can be placed either over a gate oxide and silicon or over a silicon dioxide isolation layer.

As shown in Figure 1, the devices are fabricated in a 300-nm wafer, with a die size around 25mm x 30mm. Microelectronic devices are integrated alongside the nanochannels. Photolithography and reactive ion etching are used to access the polysilicon through the metal interconnect stack. Nano-channels are etched by gas phase XeF_2 through these access holes. Due to extreme high extinction ratio of XeF_2, it is possible to etch high aspect ratio channels.

SU-8 is used to pattern fluid reservoirs on top of CMOS chips. As shown in Figure 1, by loading fluorescent dye (Texas Red), it is possible to demonstrate (a) the wetting properties of the XeF_2 etched channels and (b) the relatively low autofluorescence of the inter-metal dielectric stack.

In summary, we present the first attempt to fabricate nanofluidic channels in microelectronics CMOS chips using the polysilicon in the transistor gate as a sacrificial layer. Fluorescent molecules dissolved in water can be easily loaded into the channels and imaged with signal strength significantly over the autofluorescence of the CMOS dielectric stack.

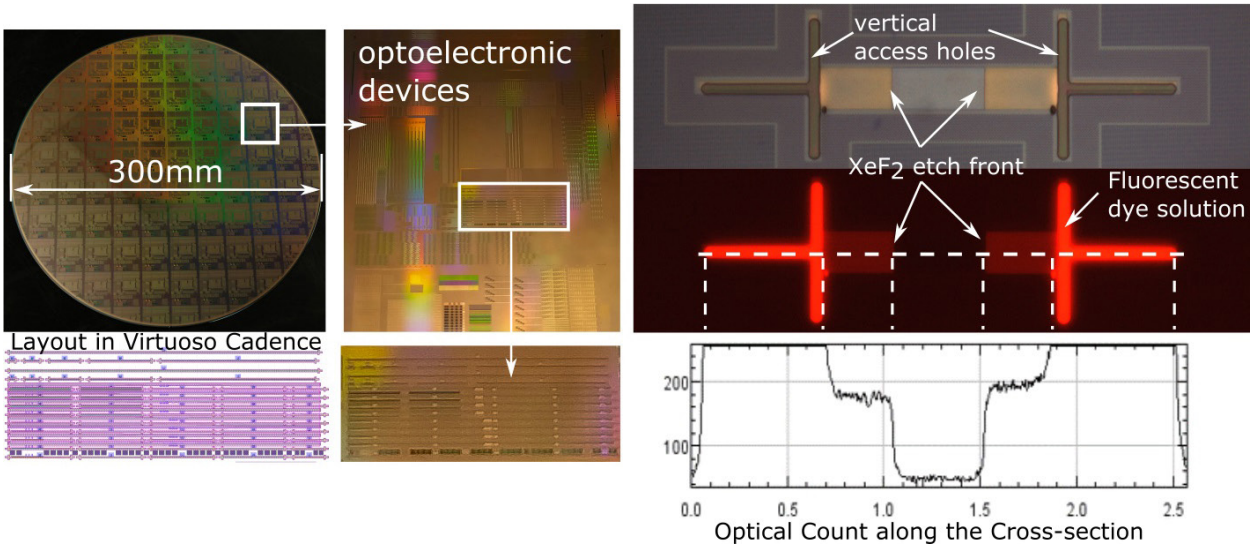

▲ Figure 1: Nanofluidics fabricated in a bulk 65-nm CMOS process on the same chip are active optoelectronic devices. The layout uses parameterized cells in Virtuoso Cadence. The nanochannel is successfully wetted by water based solution and a clear signal is visible above the autofluorescence.

FURTHER READING

- J. Rothberg, et al, "An Integrated Semiconductor Device Enabling Non-Optical Genome Sequencing," *Nature*, vol. 475, 348-352, 2011.
- C. Wang, et al, "Wafer-Scale Integration of Sacrificial Nanofluidic Chips for Detecting and Manipulating Single DNA Molecules," *Nature Communications*, vol. 8, 14243, 2017.

Capture and Concentration of Pathogens in Chaotic Flows

M. M. Alvarez, G. Trujillo de Santiago, E. Fernández-Castillo, A. Risso, G. Prakash, P. I. Sánchez-Rellstab, A. Khalilpour, A. Khademhosseini
Sponsorship: MIT- Tecnológico de Monterrey Nanotechnology Program

Infectious diseases of both viral and bacterial origin continue to be a health threat to millions of people in developed and underdeveloped countries. One successful treatment strategy for cases of sepsis or viral infections is the effective capture and removal of the pathogenic agent from the bloodstream. We are presently developing filter-less technologies for the direct capture of bacteria (i.e., *Escherichia coli*) and eventually viruses (i.e., Ebola virus-like particles).

We use a portable system for the capture of pathogens circulating through a microfluidic chamber. The system (Figure 1A) is based on the specific recognition of proteins on membranes or capsids; it integrates the use of (a) anti-pathogen polyclonal antibodies, (b) magnetic nanoparticles (MNP), (c) a microfluidic chaotic flow system, and (d) a neodymium magnet. Anti-pathogen antibodies are covalently immobilized within commercial magnetic nanoparticles to fabricate nanoparticles that will bind pathogens (Figure 1B). Our experiments compare the performance of different immobilization strategies (amino-carboxylic covalent binding and streptavidin-biotin binding) and different magnetic nanoparticle sizes (range 30 nm - 800 nm).

The heart and distinctive feature of our system is a microfluidic chamber in which the binding particles and the pathogen are mixed by the action of a laminar chaotic flow produced by the alternating rotation of two cylinders (Figure 1C). The intimate contact induced by this chaotic laminar flow promotes the capture of the pathogen by individual nanoparticles or nanoparticle clusters. The trapped pathogens are then concentrated by a simple magnet located downstream from the microchamber (Figure 2). This platform has key advantages over currently available methods, which are mostly based on the use of microfluidic channels or filtering membranes: (a) it is faster, (b) it offers superior capture due to the intimate mixing induced by the chaotic flow, and (c) it is easy to use.

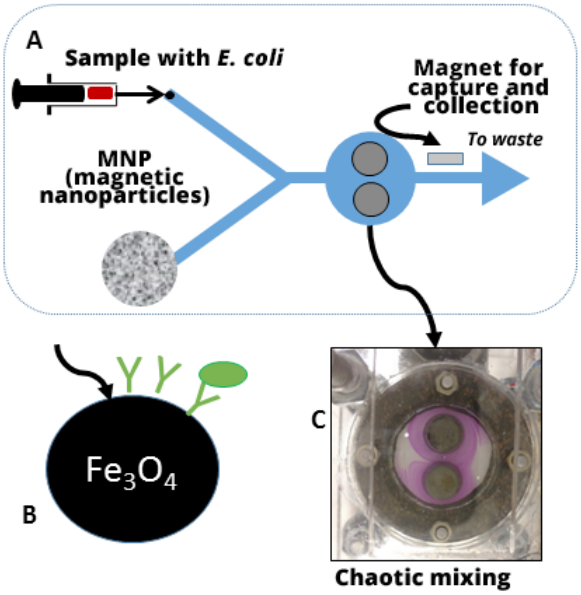

▲Figure 1: Experimental system. (a) Microfluidic system for the capture and concentration of pathogen particles (i.e., *E. coli* expressing green fluorescent protein), (b) NMP functionalized with anti-*E. coli* antibodies, (C) A chaotic flow system: the blinking vortex.

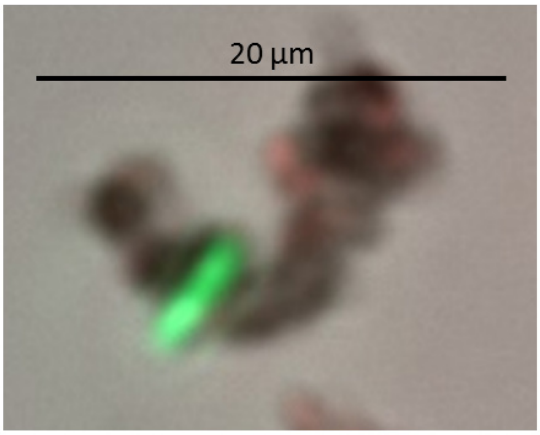

▲Figure 2: Fluorescent *E. coli* bacteria captured and concentrated in NMPs.

3-D Chaotic Printing

G. Trujillo-de Santiago, M. M. Alvarez, M. Samandari, G. Prakash, G. Chandrabhatla, B. Batzaya, P. P. S. S. Abadi, S. Mandla, R. Avery, A. Nasajpour, N. Annabi, Y. S. Zhang, A. Khademhosseini
Sponsorship: MIT-Tecnológico de Monterrey Nanotechnology Program, CONACyT, Fundación México en Harvard

Chaos has the ability to create complex and predictable structures. We use simple chaotic flows for the fabrication of complex 3-D microstructures in cross-linkable or curable liquids, using a process that we refer to as 3-D chaotic printing. We inject a drop of ink (i.e., a drop of a miscible liquid, fluorescent beads, or cells) into a viscous Newtonian liquid and then apply a chaotic mixing recipe. This generates a complex microstructure in just a few flow applications (Figure 1). This structure is then preserved with high fidelity and reproducibility by rapid crosslinking or curing of the material. The 3-D structure is the result of the rapid alignment of the injected material to the flow manifold (Figure 2). Therefore, its main features are reproducible and the overall process of fabrication is quite robust. Moreover, since the process is deterministic, it is amenable to computational modeling using computational fluid dynamics.

We currently explore applications for this technology, including the rational reinforcement of constructs by the chaotic alignment of cells and nanoparticles, the fabrication of cell-laden fibers, the development of highly complex multi-lamellar and multi-cellular tissue-like structures for biomedical applications, and the fabrication of bioinspired catalytic surfaces.

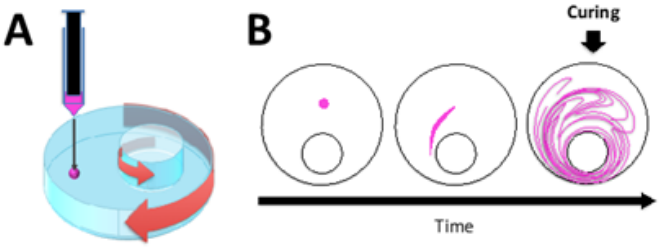

▲ Figure 1: Scheme of 3-D chaotic printing: a strategy to fabricate micro-patterned constructs using cross-linkable polymers and chaotic flows (i.e., the Journal Bearing flow), (a) a drop of "ink" (i.e., microparticles, nanoparticles, cells) is dispensed in a chaotic system, (b) after the iterative application of a chaotic recipe, a fine and complex microstructure emerges. Exposure to a curing agent freezes this microstructure.

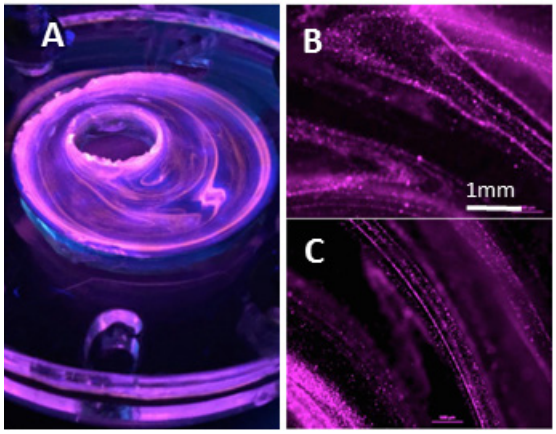

▲ Figure 2: A PDMS construct with pink fluorescent miroparticles showing a fine chaotic micropattern using the Journal Bearing flow, (a) overall view of the construct, (b & c) close-up showing the fine microstructure resulting from the application of the chaotic flow.

FURTHER READING

- M. M. Alvarez, F. J. Muzzio, S. Cerbelli, A. Adrover, and M. Giona,"Self-Similar Spatiotemporal Structure of Intermaterial Boundaries in Chaotic Flows," *Physical Review Lett.*, vol. 81, no. 16, 395-3398, 1998.
- P. D. Swanson and J. M. Ottino, "A Comparative Computational and Experimental Study of Chaotic Mixing of Viscous Fluids," *J. Fluid Mechanics,* vol. 213, 227-249, 1990.

Thin-Film Transistors for Implantable Medical Devices

Y. Hosseini, L. F. Velásquez-García, D. S. Boning
Sponsorship: TruSpine

Miniaturization and implantation of medical devices with the ability to monitor vital body parameters can enable new opportunities for medical procedures. The implantable medical devices market is estimated to grow at 5.5% compound annual growth rate (CAGR) to reach a $55B size market by 2025. In this regard, flexible hybrid electronic systems have gained attention during the last several years for deployment on various platforms such as smart lenses, cardiac implants, and brain implants, as well as in wireless modules for communication systems integrated with these implants.

In this project, we are exploring the integration of various microsystems such as sensors, thin-film transistors (TFTs), silicon microelectronics, and radio frequency identification (RFID) modules on flexible platforms (Figure 1). The goal of this project is to fabricate the essential components of these systems in a single process to reduce the integration complexity for implementing different technologies. Our initial work has focused towards integration of TFT electronics and thermal sensors on a polyimide substrate for flow sensing applications. The TFT is fabricated as a back-gate transistor, with aluminum oxide as gate insulator and indium-gallium-zinc-oxide (IGZO) as n-type channel. The thermal flow sensor consists of a combination of a heater and a resistance temperature detector (RTD) system. The thermal flow sensor consists of Au electrodes and is the extension of one of the transistor metal layers (Figure 2). This metal layer can be further extended to serve as a signal path, bonding pad, and RFID coil. Current work focuses on characterizing, optimizing, and addressing the reliability issues related to the operation of these TFTs for signal conditioning for sensing applications.

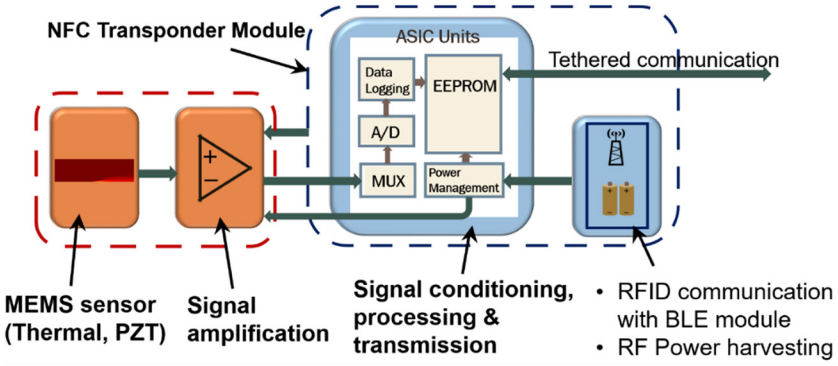

▲ Figure 1: The design outlook for integrated microsystems for sensing applications for implantable medical devices.

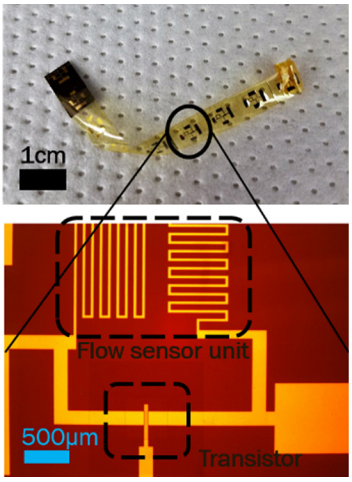

▲ Figure 2: TFTs on a flexible platform with inset image showing the integrated thermal flow sensor connection to the electronic system.

FURTHER READING

- "$54.28 Billion Implantable Medical Devices Market–Analysis and Trends & Forecasts 2016-2025." [Online]. Available: https://globenewswire.com/news-release/2017/01/24/910380/0/en/54-28-Billion-Implantable-Medical-Devices-Market-Analysis-and-Trends-Forecasts-2016-2025.html, Jan. 24, 2017.

Building Synthetic Cells for Sensing Applications

M. Hempel, E. McVay, J. Kong, T. Palacios
Sponsorship: AFOSR

Miniaturized sensors equipped with communication capabilities enable a new paradigm of sensing in areas such as health care and environmental monitoring. For example, instead of a patient measuring blood sugar by pricking a finger and analyzing a drop of blood externally, a microscopic sensor platform in the blood stream could sense the glucose concentration internally and communicate data to the outside world non-invasively.

In this project, we work towards this vision by developing a microscopic sensor platform, called a synthetic cell (SynCell) that can sense chemical substances in liquid media. The concept of our first SynCell demonstration is shown in Figure 1. After fabrication, the SynCells are lifted off and dispersed in water. Upon exposure to a specific substance, the chemical sensors onboard the SynCell are designed to permanently change their electrical resistance. Later on, they will be retrieved by using magnetic pads and analyzed externally.

To realize this concept, we designed 100-um-wide flexible polymer disk that has three chemical sensors, a stored ID number in the form of ROM transistors, and integrated magnetic readout pads as shown in Figure 2. The transistor channels and sensors are made of a single atomic layer of molybdenum disulfide (MoS2), which is a perfect material for this application because it is flexible and easy to integrate into membrane-like electronics. Furthermore, it is an excellent material to build digital electronics and very sensitive sensors.

With our first iteration of the SynCells, we demonstrated functional transistors and developed a process to lift the disks off the fabrication substrate and disperse them in solution. We also showed the ability to manipulate the SynCells with external magnetic fields. In the next steps, we want to show fully functional SynCells and demonstrate the ability to magnetically retrieve them.

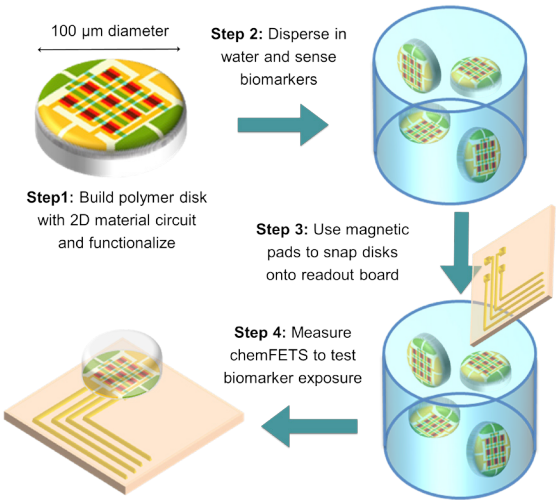

▲ Figure 1: SynCell concept of sensing an analyte in a liquid environment. After chemical exposure, the SynCell will be retrieved by magnetic pads and measured externally.

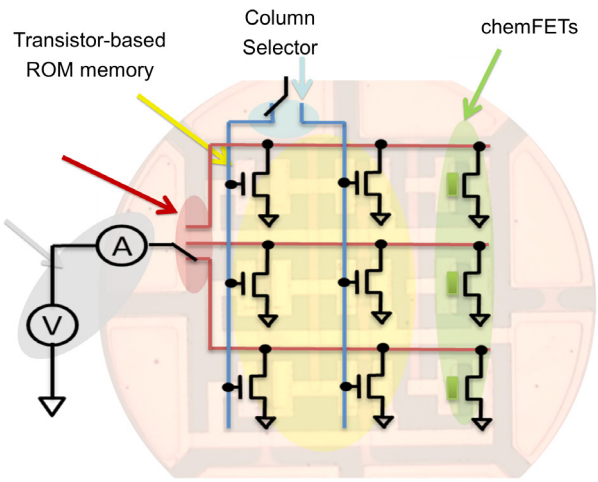

▲ Figure 2: The Syncell consists of 3 chemically sensitive transistors, as well as 6 transistors that give the cell a unique ID number for identification.

FURTHER READING

- S. S. Varghese, S. H. Varghese, S. Swaminathan, K. K. Singh, and V. Mittal, "Two-Dimensional Materials for Sensing: Graphene and Beyond," *Electronics*, vol. 4, no. 3, 651–687, Sep. 2015.
- L. Y. Chen, K. B. Parizi, H. Kosuge, M. Milaninia, M. V. McConnell, H. S. P. Wong, and A. S. Y. Poon, "Mass Fabrication and Delivery of 3-D Multilayer µTags into Living Cells," *Scientific Reports*, vol. 3, 2295, Jul. 2013.
- L. Yu et al, "Design, Modeling, and Fabrication of Chemical Vapor Deposition Grown MoS2 Circuits with E-Mode FETs for Large-Area Electronics," *Nano Lett.*, vol. 16, no. 10, 6349–6356, Oct. 2016.

Close-Packed Silicon Microelectrodes for Scalable Spatially Oversampled Neural Recording

J. Scholvin, K. Payer, C. G. Fonstad, E. S. Boyden
Sponsorship: Simons Center for the Social Brain at MIT, Paul Allen Family Foundation, NYSCF, NIH, NSF, CBMM

Two major goals of neuroscience are to understand how the activity of individual neurons yields network dynamics and how network dynamics yields behavior (and causes disease states). Reaching this goal requires innovative neuro-technologies with orders-of-magnitude improvements over traditional methods. Nanofabrication can provide the scalable technology platform necessary to record with single-spike resolution the electrical activity from a large number of individual neurons, in parallel and across different regions of the brain. By combining innovations in fabrication, design, and system integration, we can scale the number of neural recording sites: from traditionally a small number of sparse sites, to currently over 1000 high-density sites, and in the future beyond many thousands of sites distributed through many brain regions.

We designed and implemented close-packed silicon microelectrodes (Figure 1) to enable the spatially oversampled recording of neural activity (Figure 2) in a scalable fashion, using a tight continuum of recording sites along the length of the recording shank, rather than discrete arrangements of tetrode-style pads or widely spaced sites. This arrangement, thus, enables spatial oversampling continuously running down the shank, so that sorting of spikes recorded by the densely packed electrodes can be facilitated for all the sites of the probe simultaneously.

We use MEMS microfabrication techniques to create thin recording shanks and a hybrid lithography process that allows a dense array of recording sites, which we connect to with submicron-dimension wiring. We have performed neural recordings with our probes in the live mammalian brain. Figure 2 illustrates the spatial oversampling potential of closely packed electrode sites.

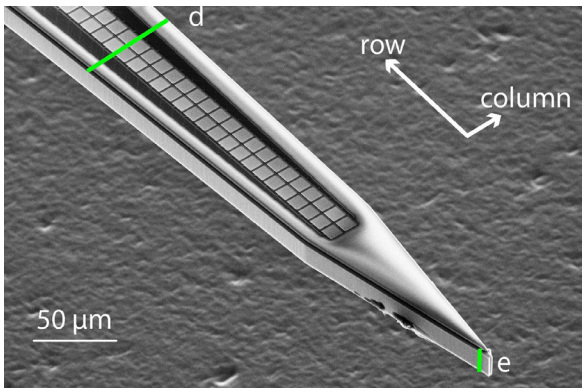

▲ Figure 1: Close-up view of the tip section of a recording shank, showing the two columns and a dense set of rows. The close-packed pads are visible as light squares in the center of the shank. Insulated metal wires connect to the individual sites, running next to the recording sites along length of the shank, visible as dark lines flanking the rows of light squares. The shank itself has a width of ~50-60 µm in the region shown (d), and is 15 µm thick (e).

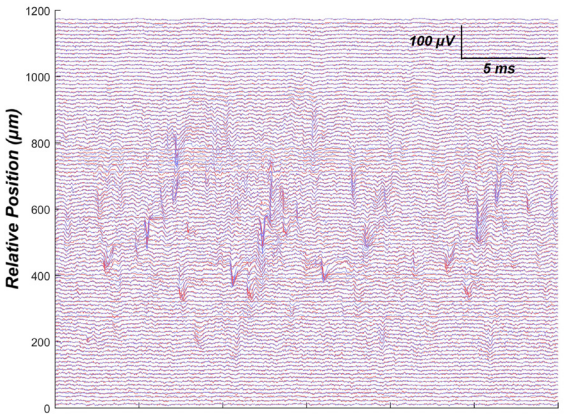

▲ Figure 2: Example of *in vivo* data from a 2-column by 102-row shank. The spatial oversampling enables spikes to be picked up by many nearby recording sites (9 x 9-µm pads, at a 10.5-µm pitch), to facilitate automated data analysis. The data shown here is a snapshot of data collected by a multi-shank, 1020-channel device.

FURTHER READING

- J. Scholvin, J. P. Kinney, J. G. Bernstein, C. Moore-Kochlacs, N. Kopell, C. G. Fonstad, and E. S. Boyden, "Close-Packed Silicon Microelectrodes for Scalable Spatially Oversampled Neural Recording," *IEEE Trans. Biomed. Eng.*, vol. 63, no. 1, 120–130, 2016.
- B. D. Allen, C. Moore-Kochlacs, J. Scholvin, J. P. Kinney, J. G. Bernstein, S. B. Kodandaramaiah, N. J. Kopell, and E. S. Boyden, "Towards Ground Truth in Ultra-Dense Neural Recording," *Computational and Systems Neuroscience (Cosyne)*, [Online]. Available: http://www.scalablephysiology.org/probes, 2016.

A Portable Bioimpedance Spectroscopy Measurement System for Congestive Heart Failure Management

M. K. Delano, C. G. Sodini
Sponsorship: MEDRC, Analog Devices, Inc.

Congestive heart failure (CHF) is a chronic medical condition that causes reduced exercise tolerance; shortness of breath; and fluid buildup in the lungs, legs, and abdomen. The disease must be managed carefully to prevent hospitalizations. While CHF-related mortality has reduced in recent years, this reduction has been accompanied by an increase in hospitalizations and readmissions. A home monitoring and management system for patients with CHF could help reduce the number of CHF-related hospitalizations and reduce the impact of CHF on the United States healthcare system.

We have developed a portable (and eventually wearable) bioimpedance spectroscopy system (BIS) to monitor fluid status levels of patients at the calf via a wearable compression sock. Our system has been evaluated in the lab and with healthy volunteers, and we are in the process of testing the system alongside a commercial BIS system (SFB7) in the hemodialysis unit at MGH to measure volume change. A wearable CHF home management system that includes our BIS system, coupled with self-tracking tools and behavior change concepts, could empower patients to more easily manage their condition and reduce the likelihood of (re)hospitalization.

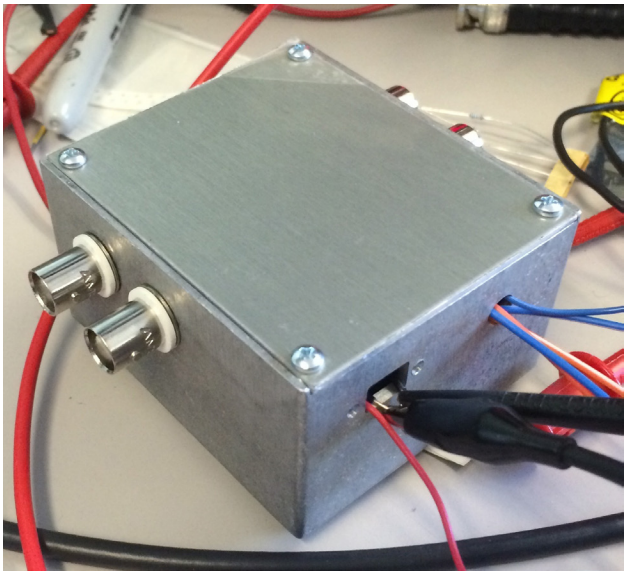

▲Figure 1: The portable bioimpedance spectroscopy measurement system inside the enclosure.

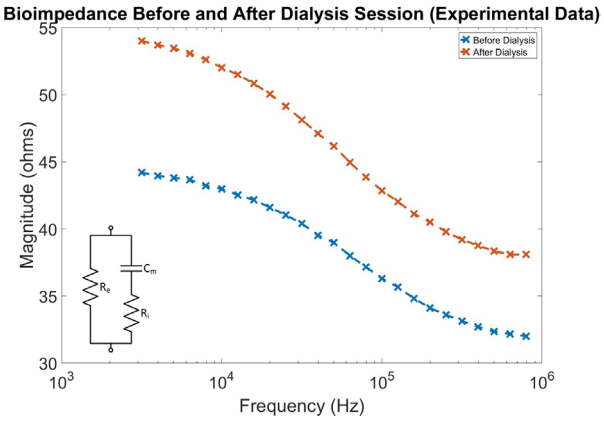

▲Figure 2: Bioimpedance spectra for a dialysis patient before (blue) and after (red) their session. Increased impedance at low frequencies implies increase Re (extracellular resistance) and decreased edema.

FURTHER READING

- M. Delano and C. G. Sodini, "A Long Term Wearable Electrocardiogram Measurement System," *Body Sensor Networks Conference*, 1-6, 2013.
- E. Winokur, M. Delano, and C. G. Sodini, "A Wearable Cardiac Monitor for Long-Term Data Acquisition and Analysis," *IEEE Transactions on Biomedical Engineering*, vol. 60, 189-92, Jan. 2013.
- D. He, E. S. Winokur, and C. G. Sodini, "An Ear-Worn Vital Signs Monitor," *IEEE Transactions on Biomedical Engineering*, vol. 62, no. 11, 2547-2552, Nov. 2015.

Wearable and Long-Term Subdermal Implantable Electroencephalograms

J. Yang, C. G. Sodini
Sponsorship: CICS

Electroencephalography (EEG) has long been used by neurologists to aid in diagnosing and treating neurological disorders ranging from sleep apnea to epilepsy. EEG can also be used as a quantitative measure of the depth of anesthesia for intensive care unit (ICU) monitoring. However, inherent difficulties still exist in capturing EEG data for extended periods of time on the order of days to weeks in humans. Such difficulties due to implementation challenges and usability lead to patient non-compliance. These challenges also curtail EEG use in clinical ICU settings due to the complexity of the setup.

This work aims to address these issues by extending the functionality and performance of a previously designed EEG ASIC. A design for a subdermal, implantable EEG recording system for long-term EEG monitoring as well as a simplified wearable EEG sensor is realized.

The implantable design is an 8-channel, 250Hz bandwidth EEG system in a 14.0mm x 15.5mm package that is wirelessly powered by an external device through inductively coupled coils with backscattering. The device is placed subdermally above the skull for continuous patient EEG monitoring for up to a month to aid neurologists with epilepsy diagnosis. This device is especially important given the severity of antiepileptic drugs' side effects. The performance of this device is verified through animal studies in pigs.

This work is also extended to the design of a wearable, wireless EEG patch for clinical settings. The device is a 20mm x 24mm, 4-channel, 250Hz bandwidth, Bluetooth low-energy (BTLE) electronics package with adhesive electrodes that can be quickly applied. This device is aimed to assist neurologists and anesthesiologists to titrate anesthetic drugs as well as more accurately monitor depth of anesthesia in operating room settings. Results are verified using patient data in clinical settings.

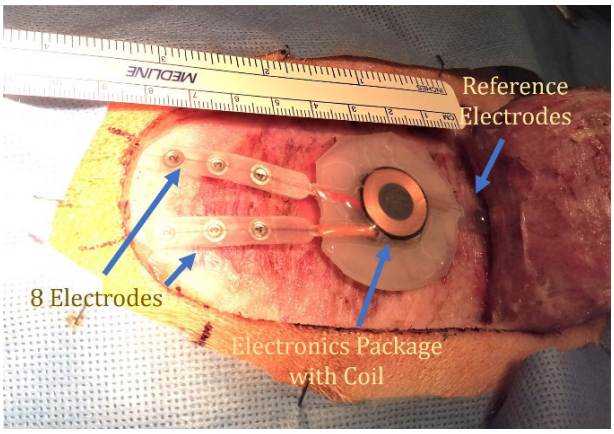

▲ Figure 1: Subdermal EEG device being implanted into a live pig model. The 8 electrodes point towards the nose of the pig; ground and reference electrodes point towards the back.

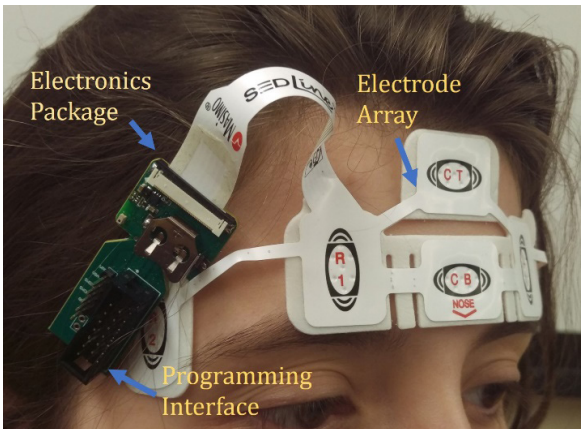

▲ Figure 2: Wearable EEG device with programmer interface board attached. The device is adhered to the user's forehead by adhesive electrodes.

Continuous and Non-Invasive Arterial Pressure Waveform Monitoring using Ultrasound

J. Seo, C. G. Sodini, H.-S. Lee
Sponsorship: Samsung Fellowship, MEDRC, Phillips

An arterial blood pressure (ABP) waveform provides valuable information for understanding cardiovascular diseases. The ABP waveform is usually obtained through an arterial line in an intensive care unit (ICU). Although considered the gold standard, this method brings the disadvantage of its invasive nature. Non-invasive methods based on vascular unloading, such as Finapres, are not suitable for prolonged monitoring due to their obstructive nature. Therefore, reliable non-invasive ABP waveform estimation has long been desired by medical communities. Medical ultrasound is an attractive imaging modality because it is inexpensive, free of ionizing radiation, and suitable for portable system implementation.

The proposed ultrasonic ABP waveform monitoring is achieved by observing the pulsatile changes of the cross-sectional area and identifying the elastic property of the arterial vessel, represented by the pulse wave velocity (PWV; the propagation speed of a pressure wave along an arterial tree) with a diastolic blood pressure measurement as a baseline. The PWV can be estimated by obtaining a flow-area plot and then measuring the slope of an initial linear region in the flow-area plot during a reflection-free period (e.g. the early systolic stage).

A prototype ultrasound device was designed to obtain a blood flow waveform and a diameter waveform simultaneously to implement the proposed technique as shown in Figure 1. A pre-clinical test was conducted on nine healthy human subjects to demonstrate the proof of concept. Figure 2 presents the comparison between the ABP waveform obtained at the middle finger with Finapres and the ABP waveform at the left common carotid artery from the prototype. The sharper ABP peaks from the Finapres are expected due to the reflection at the peripheries. Currently, the clinical study in comparison to the gold standard A-line measurement in the ICU at the hospital is being prepared.

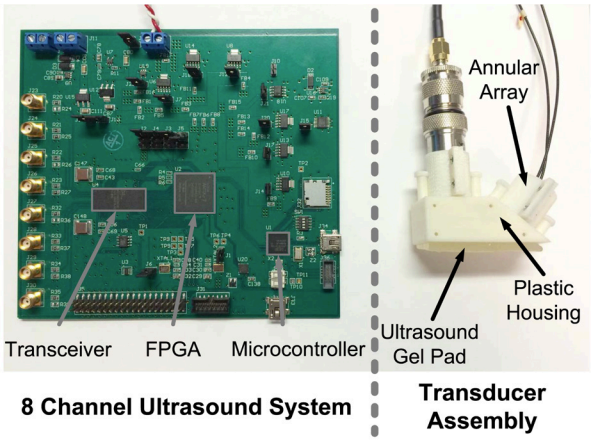

▲ Figure 1: The prototype ultrasound system and transducer assembly. The system is capable of a sufficient data rate to display blood flow and arterial pulsation simultaneously. Ultrasound gel pad is utilized to achieve acoustic coupling between the transducer surface and the skin.

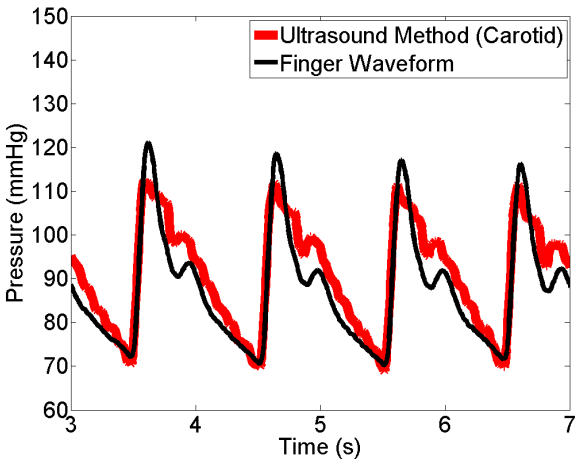

▲ Figure 2: Comparison of the estimated carotid ABP waveform to the finger ABP waveform. The finger waveform shows a sharper systolic peak due to pulse pressure amplification at peripheral arterial sites. Diastolic pressures from both methods are aligned.

FURTHER READING

- J. Seo, S. J. Pietrangelo, H.-S. Lee, and C. G. Sodini, "Carotid Arterial Blood Pressure Waveform Monitoring using a Portable Ultrasound System," *37th Annual International Conference of the IEEE Engineering in Medicine and Biology Society (EMBC)*, 5692-5695, 2015.
- J. Seo, S. J. Pietrangelo, H.-S. Lee, and C. G. Sodini, "Noninvasive Arterial Blood Pressure Waveform Monitoring using Two-Element Ultrasound System," *IEEE Transactions on Ultrasonics, Ferroelectrics, and Frequency Control*, vol. 62, no. 4, 776-784, 2015.

Three-Dimensional, Magnetic Resonance-Based Electrical Properties Mapping

J. E. C. Serrallés, A. G. Polimeridis, R. Lattanzi, D. K. Sodickson, J. K. White, L. Daniel
Sponsorship: NSF

Magnetic resonance imaging (MRI) has proven to be a safe and versatile tool in medical practice and clinical research. Clinical MRI typically relies on magnetization, T1-weighting, and T2-weighting as its contrast mechanisms. The dependence on these mechanisms is disadvantageous because these quantities are not guaranteed to vary from tissue to tissue, potentially obscuring the true contrast of the tissues. Additionally, the use of magnetization discards valuable information that describes how the scatterer interacts with fields generated by a scanner. The aim of our research is instead to use this extraneous information to generate maps of relative permittivity and conductivity, thereby significantly increasing contrast in MR images at the expense of computation time.

The task of inferring these material properties is referred to as inverse scattering, a subclass of what are called inverse problems. Inverse scattering problems typically suffer from slow convergence rates and require several full-wave electromagnetic simulations per iteration of the procedure. Our approach, called Global Maxwell Tomography, uses a volume integral equation suite, MARIE, which is custom-tailored for the typical MR setting and which results in runtimes that render the inference process tractable. Our algorithm is capable of reconstructing the known electrical properties of objects, in simulation, with use of measured MR data on the horizon. The ability to infer electrical property maps rapidly from MR data would not only improve the reliability of MRI but also pave the way for applications like automated tumor identification, patient-specific MR shimming, and real-time monitoring of heat deposition in tissue by MR coils, among others.

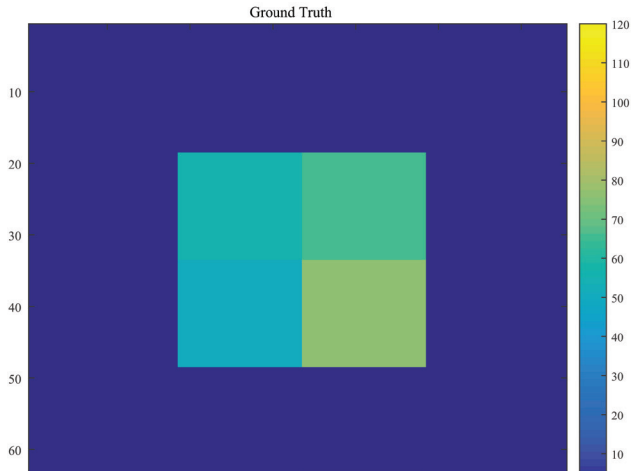

▲ Figure 1: Relative permittivity map of phantom with known electrical properties and geometry, along a central slice. This constitutes the ground truth to which the algorithm should converge.

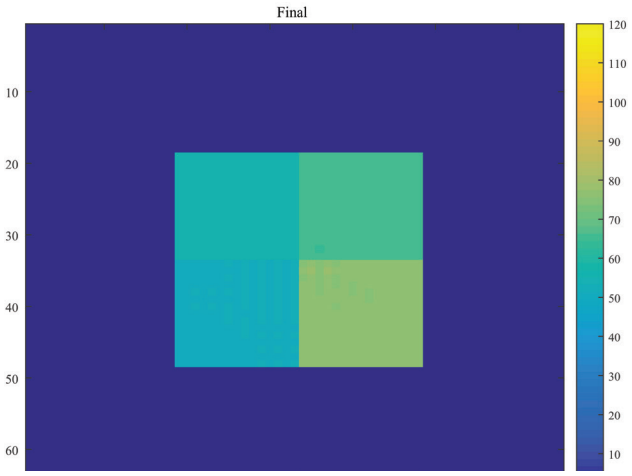

▲ Figure 2: Reconstructed relative permittivity map of the same phantom, when starting from a completely homogeneous initial guess. Reference fields are generated in simulation.

FURTHER READING

- J. E. C. Serrallés, A. G. Polimeridis, M. V. Vaidya, G. Haemer, J. K. White, D. K. Sodickson, L. Daniel, and R. Lattanzi, "Global Maxwell Tomography: A Novel Technique for Electrical Properties Mapping without Symmetry Assumptions or Edge Artifacts," presented at *ISMRM 24th Annual Meeting*, Suntec City, Singapore, May 2016.
- J. E. C. Serrallés, L. Daniel, J. K. White, D. K. Sodickson, R. Lattanzi, and A. G. Polimeridis, "Global Maxwell Tomography: A Novel Technique for Electrical Properties Mapping Based on MR Measurements and Volume Integral Equation Formulations," presented at *2016 IEEE International Symposium on AP-S–URSI National Radio Science Meeting,* Fajardo, Puerto Rico, Jun. 2016.

MARIE: A MATLAB-Based Open Source MRI Electromagnetic Analysis Software

J. F. Villena, A. Polimeridis, J. E. C. Serralles, L. Wald, E. Adalsteinsson, J. White, L. Daniel
Sponsorship: NIH, Skoltech Initiative on Computational Mathematics

Our Magnetic Resonance Integral Equation suite (MARIE) is a numerical software platform for comprehensive frequency-domain fast electromagnetic (EM) analysis of MRI systems. The tool is based on a combination of surface and volume integral equation formulations. It exploits the characteristics of the different parts of an MRI system (coil array, shield, and realistic body model), and it applies sophisticated numerical methods to rapidly perform all the required EM simulations to characterize the MRI design: computing the un-tuned coil port parameters, obtaining the current distribution for the tuned coils, and obtaining the corresponding electromagnetic field distribution in the inhomogeneous body for each transmit channel.

The underlying engine of MARIE is based on integral equation methods applied to the different domains that exist in traditional MRI problems (for example, except in interventional cases, the coil and body occupy separate spaces). The natural domain decomposition of the problem allows us to apply and exploit the best modeling engine to each domain. The inhomogeneous human body model is discretized into voxels and modeled by volume integral equation (VIE) methods. The homogeneous conductors that form the coil design and shield are tessellated into surface triangles (that allow the modeling of complex and conformal geometries), and modeled by surface integral equation (SIE) methods. Both models are coupled by applying standard dyadic Green functions. Due to the nature of integral equation methods, there is no need to model or discretize the surrounding air or non-electromagnetic materials, although the solution fields can be computed anywhere outside the discretized domain by applying the same free-space Green functions. No boundary condition needs to be defined (integral equations satisfy the radiation condition by construction), which simplifies the setting of the problem for the user: the inputs are the voxelized definition of the inhomogeneous body model, the tessellated geometry of the coil design (which the external ports defined), and the frequency of operation.

Once the models are generated, fast numerical methods are applied to solve the complete system. A set of nested iterative methods with the appropriate preconditioning is used to solve the effect of each port. Fast Fourier transform (FFT) techniques exploit the regularity of the voxelized grid and accelerate the matrix vector products. Depending on the different scenarios for analysis, some numerical models or tasks can be pre-computed to accelerate the solution, and many strategies are used to reduce either computational time or memory consumption.

The software runs on MATLAB and is able to solve a complex scattering problem in ~2-3 min. on a standard single GPU-accelerated windows desktop machine. On the same platform, it can perform a frequency sweep of a complex coil in ~3-5 min. per frequency point. Furthermore, it can solve the complete inhomogeneous body and coil system in ~5-10 min. per port, depending on the model resolution and error tolerance required. Intended to be a development platform, it includes a simple and intuitive graphic user interface (see Figure 1 for a snapshot) for standard analysis and a set of well-documented scripts to illustrate how to use the core numerical functions to perform more advanced analyses, to allow experienced users to create their own analysis by using or modifying the existing code. The input of the body is voxel-based and can be read from simple files that define position and tissue properties. The input of the coil design is based on standard triangular geometric descriptions, widely popular and with multiple open-source mesh generators available. The underlying numerical routines can be used to generate standard results, such as the B1+, B1-, and E maps presented in Figure 2, or to address other relevant problems, such as the generation of ultimate intrinsic SNR and SAR on realistic body models, fast coil design and optimization, and generation of patient-specific protocols, among others.

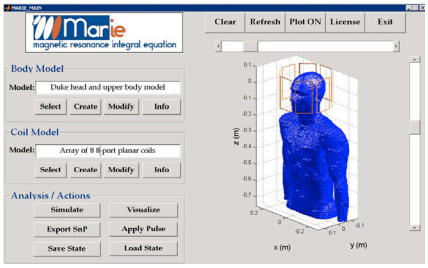

◀ Figure 1: Snapshot of MARIE's graphic user interface with body and coil models loaded, for which the simulation results are shown in Figure 2.

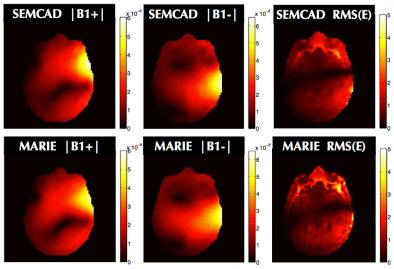

◀ Figure 2: Comparison of the (left) B1+, (center) B1-, and (right) RMS(E) maps for a body model. Top maps are with SEMCAD (SPEAG), bottom with MARIE.

FURTHER READING

- A. G. Polimeridis, J. F. Villena, L. Daniel, and J. K. White, "Stable FFT-JVIE Solvers for Fast Analysis of Highly Inhomogeneous Dielectric Objects," *J. Comp. Physics*, vol. 269, 280-296, 2014.
- A. Hochman, J. F. Villena, A. G. Polimeridis, L. M. Silveira, J. K. White, and L. Daniel, "Reduced-Order Models for Electromagnetic Scattering Problems," *IEEE Trans. on Antennas and Propagation*, vol. 62, no. 6, 3150-3162, 2014.

Automated Modeling of Large-Scale Arterial Systems

Y.-C. Hsiao, Y. Vassilevski, S. Simakov, L. Daniel
Sponsorship: MIT-Skoltech

Diagnosing medical conditions based on non-invasive (or minimally invasive) measurements requires simultaneous modeling for both local pathological arteries and global arterial networks in order to correlate the available measurements with the actual pathologies. For instance, diagnosing atherosclerosis or an aneurysm requires detailed understanding of the pressure and flow inside the bifurcation segments. Such information is typically not measurable at pathological sites but may still be attainable if it can be inferred from other measurements. Therefore, it is crucial to develop accurate yet efficient global arterial models such that the correlations between the pathologies and the available measurements can be established. The final diagnosis can be obtained by solving an inverse problem for the pathological parameters, for instance, aneurysm internal diameter, arterial wall thickness, plague stiffness, etc.

For this strategy to be effective, the model for such a large-scale arterial network must be compact, computationally tractable, and field-solver-accurate. We have proposed an innovative technique to automatically generate nonlinear dynamic models using measurement data or simulations results from partial-differential-equation (PDE) solvers, as shown in Figure 1. The generated models are guaranteed numerically stable, both when simulated alone and when interconnected within a network. This stability enables the hierarchical modeling capability, generating models for local sub-networks such as branches and bifurcations and interconnecting them to form a global network. An example of such geometry decomposition is demonstrated in Figure 2. This approach allows full exploitation of artery geometries without compromise due to the shape complexity. In addition, because the modeling efforts are subdivided into local model generations, the corresponding finite-element problems for generating training data have a tractable size. Therefore, the fluid dynamics PDEs, such as viscosity and turbulence, can be fully utilized to capture all types of nonlinearities without simplification.

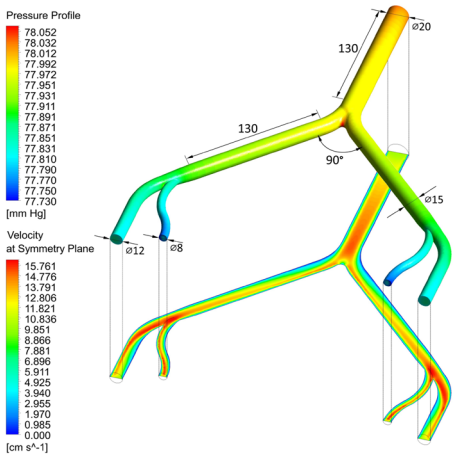

▲ Figure 1: Pressure profile (upper) and velocity profile (lower) of the human abdominal aorta and iliac arteries.

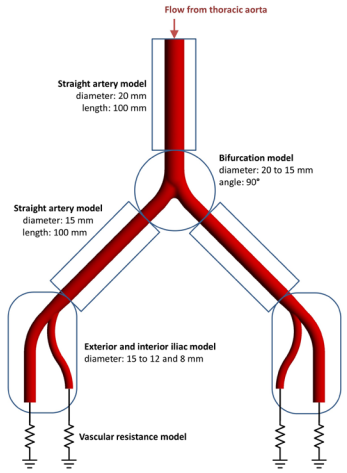

▲ Figure 2: Arterial network decomposition into local models. Each model is automatically generated using our proposed algorithm. The simulation of the overall system is accurate, efficient, and guaranteed numerically stable.

FURTHER READING

- B. Bond, T. Moselhy, and L. Daniel, "System Identification Techniques For Modeling of the Human Arterial System," in *Proc. SIAM Conference on the Life Sciences*, 12-15, 2010.
- Y.-C. Hsiao and L. Daniel, "Sparse Basis Pursuit on Automatic Nonlinear Circuit Modeling," presented at *IEEE International Conference on ASIC (ASICON)*, Shenzhen, China, 2013.

Living Materials Library

B. Datta, S. Sharma, N. Oxman, V. M. Bove, Jr.
Sponsorship: MIT Media Lab Research Consortium

The control of living systems as part of design interfaces is of interest to both the scientific and design communities due to the ability of living organisms to sense and respond to their environments. They may, for example, detect and break down harmful environmental agents or create beneficial products when environmental levels drop below a certain threshold. However, it is also important for these systems to be reversible so that the biological components are active only when their functionality is necessary, and the system can remain dormant otherwise.

The Living Material Library is an exploration of tunable hybrid systems. Our work in this area demonstrates the means through which intrinsic material properties may be functionally changed through environmental factors and, in turn, serve as dynamic substrates for living systems. Nearly all organisms have highly developed sensing capabilities and have been shown to respond behaviorally to changes in substrate properties. By creating a tunable and reversible material system, we explore how cell behavior such as adhesion, patterning, and differentiation may be influenced via an active interface.

In this iteration, we propose a reversible material system that allows for control of living interactions (much like a light switch). We are particularly interested in fluid material systems (such as electrorheological fluids) that transition from a liquid-like to a solid-like state when exposed to electric fields and currents. This endeavor brings to light the complex relationship between dynamic materials and living systems. While other methods of cell intervention often rely on light, chemicals, or temperature, here we explore substrate material properties as inputs for organisms. Our library may allow for more directed inquiry into processes such as collective cell durotaxis, general mechanotaxis, and active sensing. This marks an initial foray into establishing candidate design methods for responsive applications.

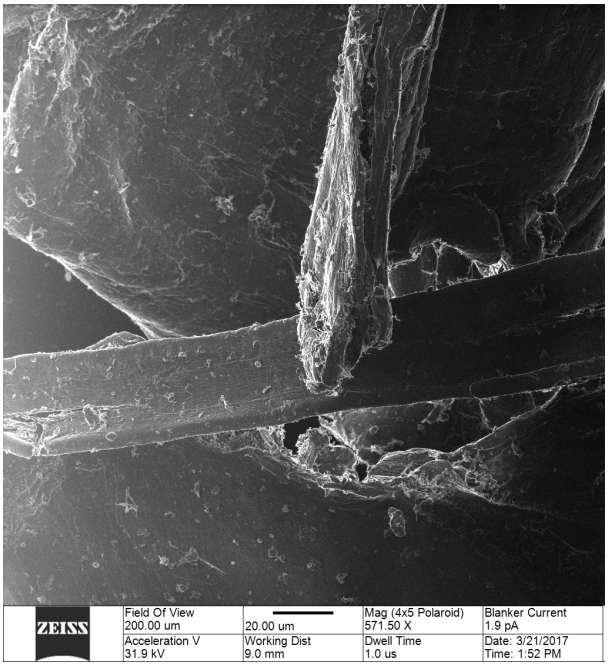

▲ Figure 1: Candidate material for responsive material substrate (helium ion micrograph of chitosan).

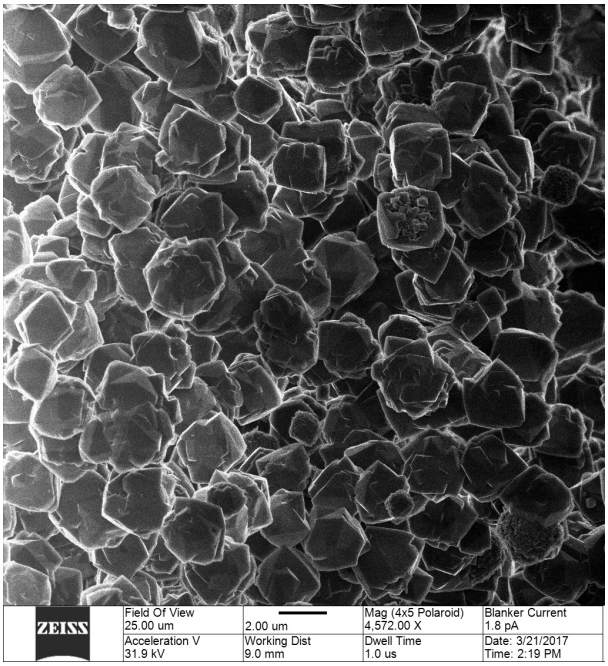

▲ Figure 2: Candidate material for responsive material substrate (helium ion micrograph of zeolite 13x).

FURTHER READING

- Y. D. Liu and H. J. Choi, "Electrorheological Fluids: Smart Soft Matter and Characteristics," *Soft Matter*, vol. 8, no. 48, 11961, 2012.
- B. Datta, S. Sharma, V. M. Bove, Jr., and N. Oxman, "Mechanosensitive Cell Behavior on Electrorheological Substrates," to be published.